

Exact 3-D Channel Impulse Response for Spherical Receivers with Arbitrary Drift Directions

Yen-Chi Lee, *Member, IEEE*, Ping-Cheng Yeh, *Member, IEEE*, and Chia-Han Lee, *Member, IEEE*

Abstract—Accurate channel modeling for spherical absorbing receivers is fundamental to the design of realistic molecular multiple-input multiple-output (MIMO) systems. While advanced modulation schemes have been proposed to mitigate interference, determining the channel impulse response (CIR) under arbitrary flow directions remains a challenge; existing exact solutions are restricted to either 1-D/no-drift scenarios or planar receiver geometries. Addressing this gap, we derive the first exact analytical CIR for a spherical receiver in a 3-D molecular communication system with uniform drift in an arbitrary direction. Unlike prior approximations that ignore the angle between the drift and the transmission axis, our approach utilizes the Girsanov theorem to analytically transform the hitting-time distribution from a stationary medium to a drifted one. The proposed closed-form expression not only eliminates modeling errors inherent in previous approximations for off-axis receivers but also enables efficient parameter-space exploration of critical system metrics (e.g., peak time and amplitude), a task that would be computationally costly with pure simulation-based approaches.

Index Terms—Molecular communication, channel modeling, multiple-input multiple-output (MIMO), advection-diffusion, stochastic differential equations.

I. INTRODUCTION

MOLECULAR Communication via Diffusion (MCvD) is a promising paradigm for nanonetworks [1], [2]. Recently, research has shifted towards molecular multiple-input multiple-output (MIMO) systems to boost data rates and reliability. Since the foundational work by Koo et al. [3], significant advances have been made in designing sophisticated modulation schemes to combat inter-link interference (ILI). For instance, Gursoy et al. [4] introduced index modulation techniques, such as molecular space shift keying (MSSK), to reduce ILI by activating fewer antennas. More recently, Ahuja and Bhatnagar [5] proposed a spatio-temporal coded modulation (MSTCM) scheme that encodes information across space and time to further mitigate interference. However, the optimization of these advanced MIMO schemes heavily relies on accurate channel coefficients (i.e., the entries of the channel matrix \mathbf{H}). Most existing studies typically resort to computationally expensive Monte Carlo simulations to obtain these coefficients, especially when the drift vector forms an arbitrary angle with the transmission link.

This work was supported by the National Science and Technology Council of Taiwan (NSTC 113-2115-M-008-013-MY3). (Corresponding author: Yen-Chi Lee.)

Y.-C. Lee is with the Department of Mathematics, National Central University, Taoyuan, Taiwan (e-mail: ycllee@math.ncu.edu.tw).

P.-C. Yeh is with the Graduate Institute of Communication Engineering, National Taiwan University, Taipei, Taiwan.

C.-H. Lee is with the Institute of Communications Engineering, National Yang Ming Chiao Tung University, Hsinchu, Taiwan.

Consequently, the literature on channel modeling has bifurcated. The first approach relies on *analytical models*. Most works approximate the channel by assuming zero drift [6] or using 1-D approximations [7], ignoring the vector nature of drift in 3-D space. While recent work [8] successfully characterized the channel impulse response (CIR) and channel capacity for *planar* receivers under drift, exact closed-form solutions for *spherical* receivers—the standard model for nanomachines—with arbitrary drift angles are still missing. This limitation forces researchers to use inaccurate channel coefficients for off-axis receivers. The second approach adopts *data-driven methods*, such as deep learning (DL) [9], to learn the channel as a black box. While effective, these methods require massive training data and lack physical explainability. A precise, physics-based model is still required to generate reliable training data or to serve as the backbone for model-based AI (e.g., deep unfolding).

TABLE I: Comparison of Analytical CIR Results in Literature. In 1-D space, the distinction between spherical and planar geometries vanishes as the receiver reduces to a point boundary.

Dim.	No Drift	Uniform Drift
$d = 1$	Lévy distribution [7], [10]	Inverse Gaussian distribution [7], [10]
$d = 3$ (Planar)	Closed-form [8]	Closed-form (Arbitrary direction solved in [8])
$d = 3$ (Spherical)	Closed-form [6]	No exact general form (Restricted to aligned drift [11])

As summarized in TABLE I, the missing case is precisely the 3-D spherical receiver with arbitrary drift. In this letter, we address this deficiency by adopting a microscopic stochastic differential equation (SDE) approach. We utilize the *Girsanov theorem* to derive a “drift factor” that analytically relates the drifted statistics to the well-known no-drift solution. To the best of our knowledge, this is the first exact analytical CIR for a fully absorbing 3-D spherical receiver under arbitrary drift direction, resolving a long-standing open modeling problem. The proposed closed-form expression not only enables the precise calculation of the full MIMO channel matrix but also facilitates the rapid characterization of critical system parameters (e.g., peak time and amplitude) across continuous parameter spaces—a task that would be computationally costly with pure simulation-based approaches.

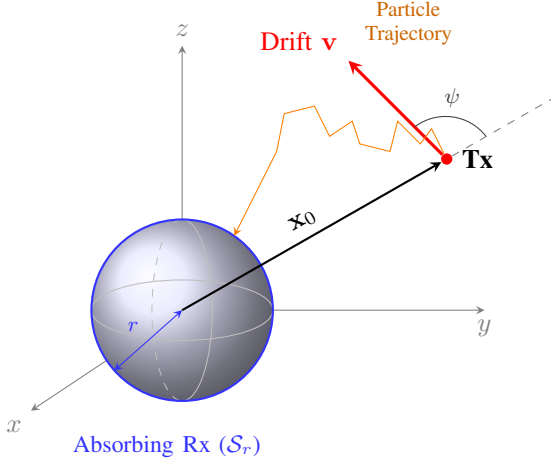


Fig. 1: System model of the 3-D molecular communication channel. A point transmitter is located at \mathbf{x}_0 , and a fully absorbing spherical receiver of radius r is at the origin. The medium is subject to a uniform drift \mathbf{v} forming an angle $\psi = \angle(\mathbf{v}, \mathbf{x}_0)$ with the position vector \mathbf{x}_0 .

II. SYSTEM MODEL

We consider an unbounded 3-D environment. The transmitter (Tx) is a point source located at position $\mathbf{x}_0 \in \mathbb{R}^3$. The receiver (Rx) is a fully absorbing sphere of radius r centered at the origin, denoted by \mathcal{S}_r . We assume $|\mathbf{x}_0| > r$.

Information particles are released at $t = 0$. We adopt a microscopic viewpoint where the trajectory of a single particle \mathbf{X}_t follows an *Itô process* [12]:

$$d\mathbf{X}_t = \mathbf{u}(t)dt + \sigma d\mathbf{B}_t, \quad (1)$$

$$\mathbf{X}_0 = \mathbf{x}_0, \quad (2)$$

where $\mathbf{u}(t)$ represents the instantaneous drift vector (e.g., due to background flow and electric fields), $\sigma = \sqrt{2D}$ accounts for the diffusion coefficient D , and \mathbf{B}_t is the standard 3-D Brownian motion. While our framework supports time-varying drift satisfying the Novikov condition, we focus in this letter on the case of *constant uniform drift* $\mathbf{u}(t) \equiv \mathbf{v}$ to derive explicit closed-form solutions.

The CIR, denoted as $f_d^{(v)}(t)$, is defined as the probability density function (PDF) of the first hitting time

$$T = \inf\{t > 0 : |\mathbf{X}_t| = r\}. \quad (3)$$

Unlike PDE approaches, which are often intractable for arbitrary drift with absorbing boundaries, the SDE framework captures the *hitting position*. This spatial information is key to solving the problem via measure transformation.

III. DERIVATION OF THE DRIFTED CIR

To provide a clear roadmap of our methodology, we illustrate the derivation flow in Fig. 2. Our strategy bridges the gap between existing no-drift solutions and the general drifted case by leveraging measure theory.

To derive the exact CIR under arbitrary drift, relying solely on the marginal hitting-time distribution for the no-drift case [6] is insufficient, as the advection effect depends heavily

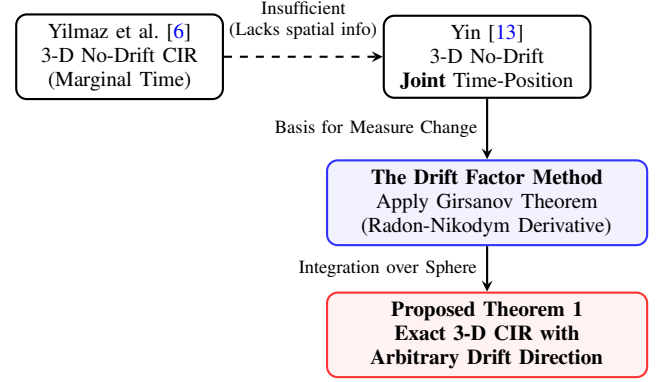


Fig. 2: Derivation flow of the proposed method. We start from Yin's joint distribution [13] and apply the Girsanov theorem to derive the general solution.

on the specific hitting location on the spherical boundary. Therefore, our approach begins with the *joint probability density* of the hitting time T and hitting position \mathbf{X}_T for a zero-drift Brownian motion, denoted as $f_d(t, \mathbf{y})$ where $\mathbf{y} \in \mathcal{S}_r$ [13].

We employ the Girsanov theorem to perform a change of measure from the zero-drift process (measure \mathbb{Q}) to the drifted process (measure \mathbb{P}). This transformation introduces a *drift factor*—the Radon-Nikodym derivative evaluated at the hitting time—which analytically relates the drifted statistics to the known zero-drift joint density

$$f_d^{(v)}(t, \mathbf{y}) = \underbrace{\exp\left(\frac{\mathbf{v} \cdot (\mathbf{y} - \mathbf{x}_0)}{\sigma^2} - \frac{|\mathbf{v}|^2 t}{2\sigma^2}\right)}_{\text{Drift Factor}} \times f_d(t, \mathbf{y}). \quad (4)$$

The exact CIR, $f_d^{(v)}(t)$, is defined as the marginal distribution of the hitting time, obtained by integrating the drifted joint PDF over the spherical surface \mathcal{S}_r :

$$f_d^{(v)}(t) = \int_{\mathcal{S}_r} \underbrace{e^{\frac{\mathbf{v} \cdot (\mathbf{y} - \mathbf{x}_0)}{\sigma^2} - \frac{|\mathbf{v}|^2 t}{2\sigma^2}}}_{\text{Drift Factor}} f_d(t, \mathbf{y}) ds(\mathbf{y}). \quad (5)$$

The term $e^{-|\mathbf{v}|^2 t / 2\sigma^2 - \mathbf{v} \cdot \mathbf{x}_0 / \sigma^2}$ is independent of \mathbf{y} and can be pulled out of the integral. The core mathematical challenge lies in integrating the spatial coupling term $e^{\mathbf{v} \cdot \mathbf{y} / \sigma^2}$ against the infinite series expansion of $f_d(t, \mathbf{y})$ provided in [13].

We utilize the following key identity (extended from [13, Lemma 2.5]) to resolve the surface integral for each mode m :

Lemma 1. For any vector $\mathbf{c} \in \mathbb{R}^d$,

$$\begin{aligned} & \int_{\mathcal{S}_r} e^{\mathbf{c} \cdot \mathbf{y}} C_m^h(\cos \angle(\mathbf{x}_0, \mathbf{y})) ds(\mathbf{y}) \\ &= 2(r\pi)^{\frac{d}{2}} \left(\frac{|\mathbf{c}|}{2}\right)^{-h} I_{m+h}(|\mathbf{c}|r) C_m^h(\cos \angle(\mathbf{c}, \mathbf{x}_0)). \end{aligned} \quad (6)$$

We apply Lemma 1 by setting $\mathbf{c} = \mathbf{v} / \sigma^2$. Consequently, the angle term becomes $\angle(\mathbf{c}, \mathbf{x}_0) = \angle(\mathbf{v}, \mathbf{x}_0) = \psi$. By substituting the series expansion of $f_d(t, \mathbf{y})$ into (5) and interchanging the order of summation and integration, the CIR

calculation reduces to a term-by-term application of Lemma 1. Namely,

$$f_d^{(v)}(t) = \mathcal{K}(t) \sum_{m=0}^{\infty} \mathcal{T}_m(t) \times \underbrace{\int_{S_r} e^{\frac{\mathbf{v} \cdot \mathbf{y}}{\sigma^2}} C_m^h(\cos \angle(\mathbf{x}_0, \mathbf{y})) ds(\mathbf{y})}_{\text{Solved by Lemma 1}}, \quad (7)$$

where $\mathcal{K}(t)$ accounts for the drift constants and $\mathcal{T}_m(t)$ represents the time-dependent coefficients from the zero-drift solution. The integral in (7) yields the modified Bessel function term $I_{m+h}(|\mathbf{v}|r/\sigma^2)$ and the directional component $C_m^h(\cos \psi)$. Combining these factors leads to the final exact closed-form solution.

Theorem 1 (Exact CIR for Arbitrary Drift). *For d -dimensional space, the exact CIR with uniform drift \mathbf{v} is given by*

$$f_d^{(v)}(t) = -e^{-\frac{\mathbf{v} \cdot \mathbf{x}_0}{\sigma^2} - \frac{|\mathbf{v}|^2 t}{2\sigma^2}} \frac{2^{h+1} \Gamma(h+1) \sigma^{2h}}{\pi(|\mathbf{v}||\mathbf{x}_0|)^h} \times \sum_{m=0}^{\infty} (m+h) I_{m+h} \left(\frac{|\mathbf{v}|r}{\sigma^2} \right) C_m^h(\cos \psi) \times \int_0^{\infty} \frac{\lambda Z_{m+h}(|\mathbf{x}_0|/r, \lambda r/\sigma)}{J_{m+h}^2(\lambda r/\sigma) + Y_{m+h}^2(\lambda r/\sigma)} e^{-\frac{1}{2} \lambda^2 t} d\lambda, \quad (8)$$

where $\psi = \angle(\mathbf{v}, \mathbf{x}_0)$ is the angle between the drift vector and the initial position vector, $h = (d-2)/2$, and $I_\nu(\cdot)$ denotes the modified Bessel function of the first kind.

IV. NUMERICAL RESULTS AND DISCUSSION

In this section, we validate the derived analytical formula against particle-based Monte Carlo (MC) simulations and utilize the proposed closed-form solution to characterize critical channel metrics. All simulations are performed using MATLAB (R2025b). To ensure consistency with established channel modeling literature [6], the default system parameters are: diffusion coefficient $D = 80 \mu\text{m}^2/\text{s}$, receiver radius $r = 10 \mu\text{m}$, and initial distance $|\mathbf{x}_0| = 20 \mu\text{m}$. We investigate two drift velocity scenarios: moderate drift ($|\mathbf{v}| = 5 \mu\text{m}/\text{s}$) and strong drift ($|\mathbf{v}| = 10 \mu\text{m}/\text{s}$).

A. Validation against Monte Carlo Simulations

The validation results for the channel impulse response (CIR) are presented in Fig. 3. The figure compares the analytical predictions (Eq. 8, truncated at $m = 30$) with MC histograms ($N_{tx} = 10^6$) across three drift angles: positive ($\psi = 180^\circ$), perpendicular ($\psi = 90^\circ$), and negative ($\psi = 0^\circ$).

The top row (Figs. 3(a)-(c)) depicts the case of moderate drift ($|\mathbf{v}| = 5 \mu\text{m}/\text{s}$), while the bottom row (Figs. 3(d)-(f)) shows the strong drift case ($|\mathbf{v}| = 10 \mu\text{m}/\text{s}$). As observed, the analytical curves exhibit excellent agreement with the simulations in all scenarios. Comparing the two rows reveals the impact of advection: for positive drift (a vs. d), increasing velocity significantly sharpens the pulse and advances the arrival time. Conversely, for negative drift (c vs. f), a higher

velocity severely suppresses the tail, making signal detection challenging. Quantitatively, across all evaluated scenarios, the analytical expression matches the simulations with a normalized root-mean-square error (NRMSE) consistently below 4%, where NRMSE is computed by normalizing the RMSE by the peak amplitude of the simulated CIR. Additional validation with varying receiver radii ($r \in [5, 15] \mu\text{m}$) and drift magnitudes ($|\mathbf{v}| \in [5, 20] \mu\text{m}/\text{s}$), omitted due to space constraints, confirms that the analytical expression maintains excellent agreement across a wide parameter range. We emphasize that since Theorem 1 is derived from first principles (the SDE model) without geometric approximations, Eq. (8) represents the exact theoretical ground truth; thus, any residual discrepancy is attributable strictly to the stochastic variance of finite-particle simulations, which vanishes asymptotically in accordance with the Law of Large Numbers.

B. Characterization of Peak Metrics

Deriving a closed-form expression for the peak time t_{peak} is analytically intractable due to the complexity of the series solution in (8). Furthermore, extracting precise peak metrics via particle-based simulations is often computationally prohibitive, as it requires averaging over massive ensembles to suppress stochastic noise. Our analytical model resolves this challenge by providing a smooth, exact objective function that allows for rapid and precise numerical maximization. Notably, the analytical evaluation of (8) is typically 10^3 – 10^4 times faster than equivalent Monte Carlo estimation.

Fig. 4 illustrates the dependency of peak metrics on system parameters. Fig. 4(a) quantifies the impact of drift velocity, highlighting the exponential signal suppression observed under negative drift ($\psi = 0^\circ$). Fig. 4(b) reveals the geometric impact of the receiver size. It is observed that while the peak amplitude grows quadratically with the absorbing surface area, the peak time t_{peak} decreases monotonically as the receiver radius r increases. This advancement in arrival time is consistent across all drift directions and is primarily driven by the reduction in the effective transmission distance ($|\mathbf{x}_0| - r$).

V. CONCLUSION

This letter presents the first exact analytical CIR for 3-D spherical receivers under arbitrary drift. By leveraging the Girsanov theorem, we derive a closed-form solution that generalizes zero-drift statistics to advective environments, providing a rigorous foundation for molecular MIMO channel matrices. The proposed model enables rapid sensitivity analysis of system metrics without computationally intensive simulations. Furthermore, the derived measure change suggests potential applicability to passive receivers [14], [15], offering a pathway to generalize current 1-D flow results to 3-D geometries.

REFERENCES

- [1] I. F. Akyildiz, F. Brunetti, and C. Blázquez, "Nanonetworks: A new communication paradigm," *Computer Networks*, vol. 52, no. 12, pp. 2260–2279, 2008.
- [2] T. Nakano, A. Eckford, and T. Haraguchi, *Molecular Communication*. Cambridge University Press, 2013.

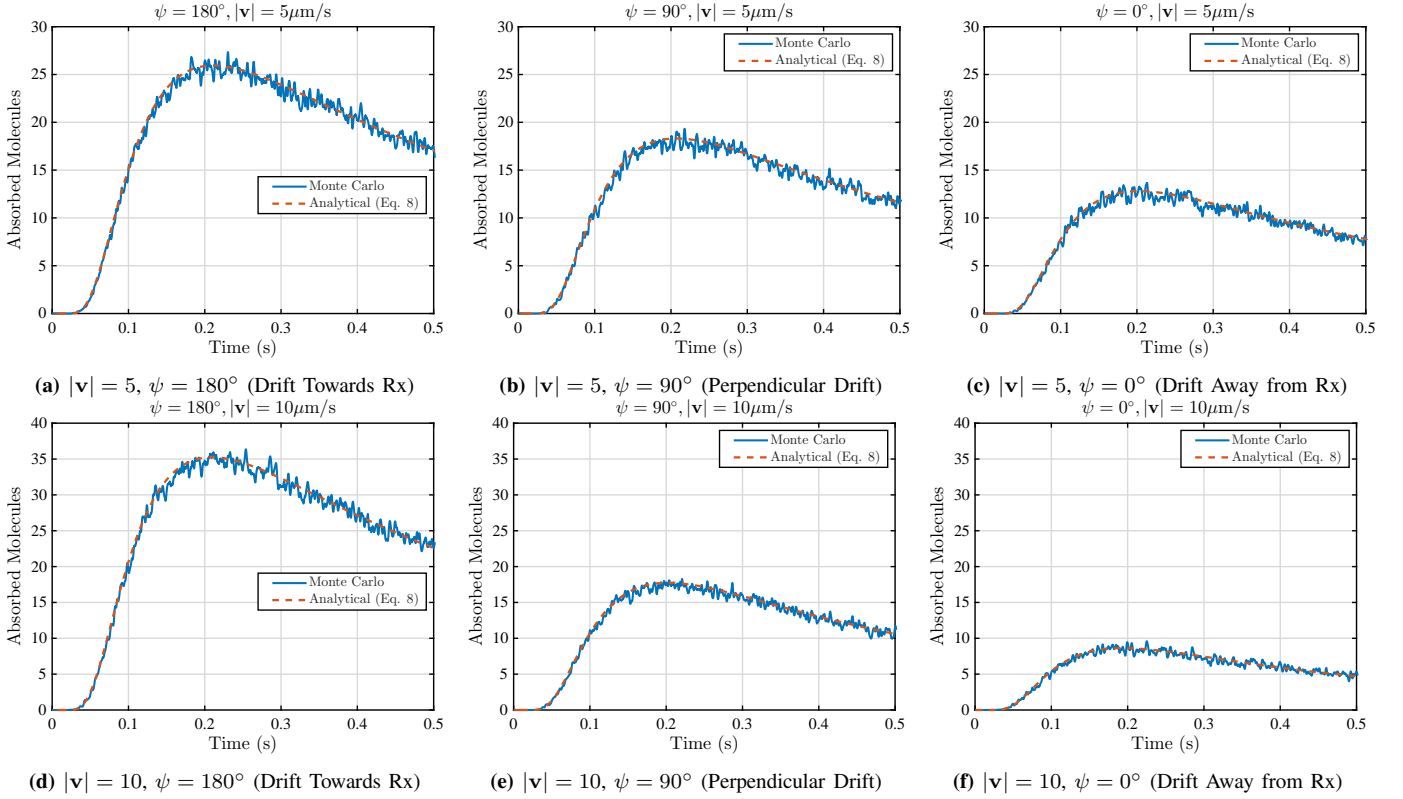


Fig. 3: Validation of analytical CIR against Monte Carlo simulations. **Top Row:** Moderate drift ($|\mathbf{v}| = 5 \mu\text{m/s}$). **Bottom Row:** Strong drift ($|\mathbf{v}| = 10 \mu\text{m/s}$). Columns correspond to positive ($\psi = 180^\circ$), perpendicular ($\psi = 90^\circ$), and negative ($\psi = 0^\circ$) drift directions.

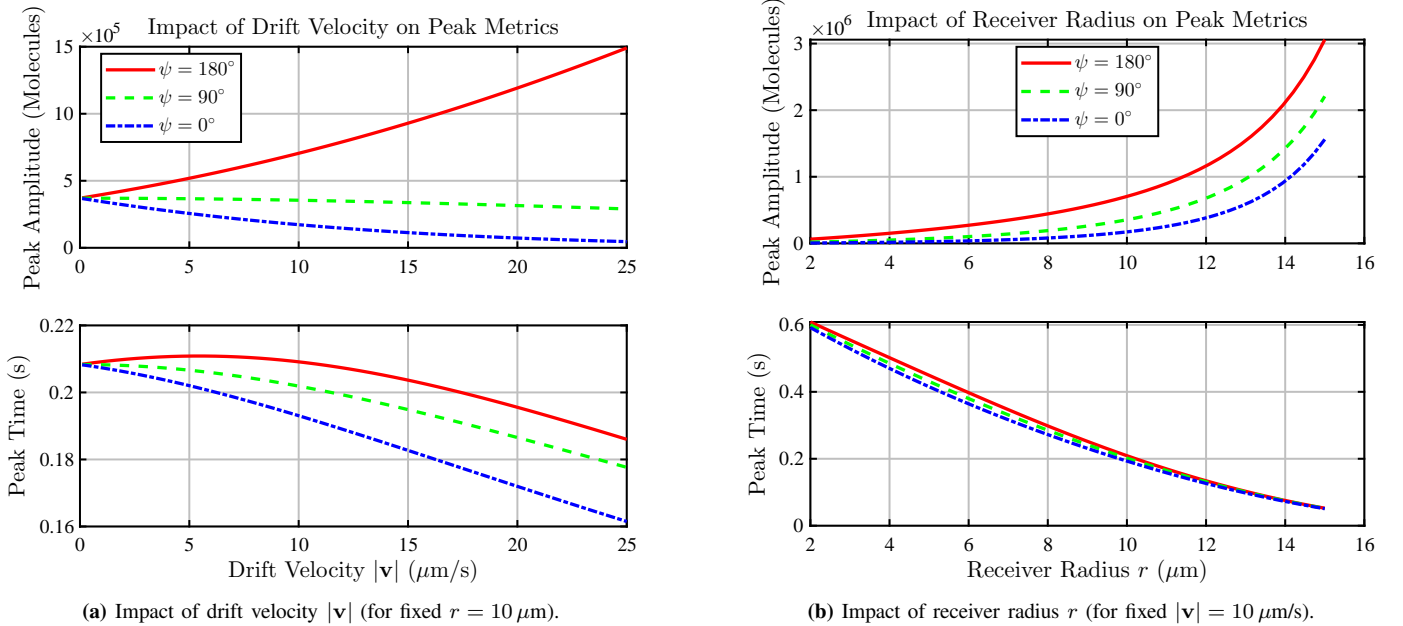


Fig. 4: Analytical characterization of peak amplitude (top panels) and peak time (bottom panels). (a) Dependency on drift velocity magnitude. (b) Dependency on receiver radius. The continuous curves demonstrate the model's capability to efficiently sweep parameter spaces, revealing distinct sensitivities for different drift angles ψ .

- [3] B.-H. Koo, C. Lee, H. B. Yilmaz, N. Farsad, A. W. Eckford, and C.-B. Chae, "Molecular MIMO: From theory to prototype," *IEEE Journal on Selected Areas in Communications*, vol. 34, no. 3, pp. 600–614, 2016.
- [4] M. C. Gursoy, E. Basar, A. E. Pusane, and T. Tugcu, "Index modulation for molecular communication via diffusion systems," *IEEE Transactions on Communications*, vol. 67, no. 5, pp. 3337–3350, May 2019.
- [5] M. Ahuja and M. R. Bhatnagar, "Performance analysis and receiver design of spatio-temporal coded modulation scheme for diffusion-based molecular MIMO systems," *IEEE Transactions on Molecular, Biological*

- and Multi-Scale Communications*, vol. 8, no. 3, pp. 119–137, Sep. 2022.
- [6] H. B. Yilmaz, A. C. Heren, T. Tugcu, and C.-B. Chae, "Three-dimensional channel characteristics for molecular communications with an absorbing receiver," *IEEE Communications Letters*, vol. 18, no. 6, pp. 929–932, 2014.
- [7] K. V. Srinivas, A. W. Eckford, and R. S. Adve, "Molecular communication in fluid media: The additive inverse Gaussian noise channel," *IEEE Transactions on Information Theory*, vol. 58, no. 7, pp. 4678–4692, 2012.

- [8] Y.-C. Lee, Y.-F. Lo, J.-M. Wu, and M.-H. Hsieh, "Characterizing first arrival position channels: Noise distribution and capacity analysis," *IEEE Transactions on Communications*, vol. 72, no. 7, pp. 4010–4025, Jul. 2024.
- [9] N. Farsad and A. Goldsmith, "Neural network detection for data-driven signal processing in molecular communication networks," *IEEE Transactions on Molecular, Biological and Multi-Scale Communications*, vol. 4, no. 3, pp. 143–158, 2018.
- [10] S. Kadloor, R. S. Adve, and A. W. Eckford, "Molecular communication using Brownian motion with drift," *IEEE Transactions on NanoBioScience*, vol. 11, no. 2, pp. 89–99, 2012.
- [11] B. C. Akdeniz, H. B. Yilmaz, A. E. Pusane, and T. Tugcu, "Impulse response of 3-D molecular communication," in *Proceedings of the 3rd Workshop on Molecular Communications*, Ghent, Belgium, Apr. 2018.
- [12] O. Calin, *An Informal Introduction to Stochastic Calculus with Applications*. Singapore: World Scientific, 2015.
- [13] C. Yin and C. Wang, "Hitting time and place of Brownian motion with drift," *The Open Statistics and Probability Journal*, vol. 1, pp. 38–42, 2009.
- [14] A. Noel, Y. Deng, D. Makrakis, and A. Hafid, "Active versus passive: Receiver model transforms for diffusive molecular communication," in *Proc. IEEE Global Commun. Conf. (GLOBECOM)*, Washington, DC, USA, Dec. 2016, pp. 1–6.
- [15] M. Pierobon and I. F. Akyildiz, "Diffusion-based noise analysis for molecular communication in nanonetworks," *IEEE Trans. Signal Process.*, vol. 59, no. 6, pp. 2532–2547, Jun. 2011.

APPENDIX A

THEORETICAL CONSISTENCY AND PHYSICAL LIMITS

In this appendix, we demonstrate that the derived 3-D framework is self-consistent and implies the classical 1-D results as a special case. We also discuss the physical implications of the total hitting probability in 3-D space.

A. Reduction to 1-D Inverse Gaussian Distribution

Consider the 1-D limit where the spherical receiver S_r collapses to a point boundary, and the transmitter is located at distance $d = |\mathbf{x}_0|$. In the absence of drift, the first hitting time PDF is given by the well-known Lévy distribution. Using the diffusion coefficient D (where $\sigma^2 = 2D$), it can be expressed as

$$f_{1D}^{(0)}(t) = \frac{d}{\sqrt{4\pi Dt^3}} \exp\left(-\frac{d^2}{4Dt}\right). \quad (9)$$

From Section III, the Radon-Nikodym derivative (drift factor) transforming the measure from a zero-drift process to one with uniform drift \mathbf{v} is

$$\mathcal{L}(t) = \exp\left(\frac{\mathbf{v} \cdot (\mathbf{y} - \mathbf{x}_0)}{2D} - \frac{|\mathbf{v}|^2 t}{4D}\right). \quad (10)$$

In the 1-D case with drift velocity v directed towards the receiver, we implicitly use the fact that on the hitting event, the particle's position \mathbf{y} is fixed at the absorbing boundary. Thus, the displacement is deterministic: $\mathbf{v} \cdot (\mathbf{y} - \mathbf{x}_0) = vd$. The drift factor simplifies to $\exp\left(\frac{vd}{2D} - \frac{v^2 t}{4D}\right)$.

Multiplying the zero-drift PDF (9) by this factor yields the drifted PDF:

$$\begin{aligned} f_{1D}^{(v)}(t) &= f_{1D}^{(0)}(t) \times \mathcal{L}(t) \\ &= \frac{d}{\sqrt{4\pi Dt^3}} \exp\left(-\frac{d^2}{4Dt} + \frac{vd}{2D} - \frac{v^2 t}{4D}\right) \\ &= \frac{d}{\sqrt{4\pi Dt^3}} \exp\left(-\frac{(d - vt)^2}{4Dt}\right). \end{aligned} \quad (11)$$

Letting $\lambda = d^2/2D$ and $\mu = d/v$, this expression becomes

$$f_{1D}^{(v)}(t) = \sqrt{\frac{\lambda}{2\pi t^3}} \exp\left(-\frac{\lambda(t - \mu)^2}{2\mu^2 t}\right). \quad (12)$$

This recovers exactly the *Inverse Gaussian distribution*, validating the consistency of our measure transformation approach with established 1-D literature [7].

B. 3-D Total Hitting Probability

A key distinction between 1-D and 3-D diffusion is the recurrence property. Unlike 1-D Brownian motion, which is recurrent (hitting probability is 1), 3-D diffusion is transient.

By integrating our exact CIR expression over $t \in [0, \infty)$, or equivalently solving the steady-state advection-diffusion equation $D\nabla^2 P - \mathbf{v} \cdot \nabla P = 0$ with absorbing boundary conditions, we obtain the total hitting probability. Specifically, for the scenario where the drift vector is anti-parallel to the transmitter-receiver direction (i.e., pointing away from the receiver with $\psi = 0^\circ$), the probability becomes

$$\mathbb{P}(T < \infty) = \underbrace{\frac{r}{|\mathbf{x}_0|}}_{\text{Geometric}} \times \underbrace{\exp\left(-\frac{|\mathbf{v}|(|\mathbf{x}_0| - r)}{D}\right)}_{\text{Advective Decay}}. \quad (13)$$

This result highlights that signal loss in 3-D is governed by two factors: the geometric dilution ratio $r/|\mathbf{x}_0|$ (which exists even when $|\mathbf{v}| = 0$) and the exponential suppression due to adverse drift. Neither factor is fully captured by standard 1-D approximations, underscoring the necessity of the proposed 3-D model.